The Astronomical Journal, 164:221 (11pp), 2022 November https://doi.org/10.3847/1538-3881/ac9610

Search for an Alien Message to a Nearby Star

Michaël Gillon[1], Artem Burdanov[2], and Jason T. Wright[3]
[1] Astrobiology Research Unit, University of Liège, Allée du 6 août 19C, B-4000 Liège, Belgium; michael.gillon@uliege.be
[2] Department of Earth, Atmospheric and Planetary Science, Massachusetts Institute of Technology, 77 Massachusetts Avenue, Cambridge, MA 02139, USA
[3] Penn State Extraterrestrial Intelligence Center, 525 Davey Laboratory, The Pennsylvania State University, University Park, PA 16802, USA
Received 2022 September 9; accepted 2022 September 27; published 2022 October 27

Abstract

If alien probes have colonized the whole galaxy, they could have formed an efficient galactic-scale communication network by establishing direct gravitationally lensed links between neighboring systems. Under this scenario, observing the positions opposite the nearest ecliptic stars represents a promising artifact SETI strategy that could make it possible to "eavesdrop" on the emission of local probes to one of these stars. In this context, we present here a first attempt to detect optical messages emitted from the solar system to the ecliptic star Wolf 359, the third-nearest stellar system, based on observations gathered by the TRAPPIST-South and SPECULOOS-South robotic telescopes. While sensitive enough to detect constant emission with emitting power as small as a few watts, this search led to a null result. We note that the putative alien probes could be emitting "off-axis" and be located much closer to the Sun than the start of the "solar gravitational line" at 550 au. We performed a search for such an off-axis emitter in our data, whose result turned out negative too.

Unified Astronomy Thesaurus concepts: Astrobiology (74); Technosignatures (2128); Search for extraterrestrial intelligence (2127)

1. Introduction

Gillon (2014, hereafter G14) hypothesized that if the Milky Way had been colonized/explored by interstellar probes (Freitas 1980; Valdes & Freitas 1980), they could have formed an efficient and dynamical galactic-scale communication network by direct links between neighboring systems, using stars as gravitational lenses (GLs; von Eshleman 1979; Maccone 1994). Under this hypothesis, alien Focal Interstellar Communication Devices (FICDs) could be present in our solar system, in the focal region of some of the nearest stars, at more than 550 au from the Sun. Based on this hypothesis, G14 proposed a novel search for extraterrestrial intelligence (SETI; Tarter 2001) strategy consisting in the intense multispectral monitoring of the focal regions of the nearest stars, with the hope of catching a communication leakage from the FICDs. This strategy has been explored further by subsequent studies (Gertz 2018, 2021; Hippke 2020a, 2020b, 2021; Kerby & Wright 2021; Marcy et al. 2022). Notably, Kerby & Wright (2021) examined the engineering requirements of the GL-based interstellar communication method, showing that modern propulsion systems should enable FICDs to maintain their interstellar communication link over century-long timescales provided that their host stars are relatively unperturbed (e.g., by a stellar companion).

In this paper, we focus on the possibility of detecting the *interstellar* messages from a specific FICD (vs. its *local* communications with probes in the solar system, as was recently attempted by Marcy et al. 2022). We identify Wolf 359, the third-nearest stellar system, as the best target for such a search, and we present a first attempt to detect optical messages emitted from the solar system to this star.

2. Attempting to Detect an Interstellar Message from an Alien FICD: Practical Considerations

A first element to consider for the envisioned search is the spectral range. Because of the refractive and scattering effects of its plasma, the solar corona acts on photons grazing the Sun as a divergent lens opposing the effect of the solar gravity (von Eshleman 1979; Turryshev & Anderson 2003; Galea & Swinney 2011; Hippke 2021). This deflection effect is especially strong for radio waves. It can be modeled by the following formula relating the divergent deflection angle $\theta_{\rm pl}$ to the impact parameter b (in solar radius $R_\odot$) and frequency ν of the photons:

$$\theta_{\rm pl}(b,\nu) = \left(\frac{\nu_0}{\nu}\right)^2 [2952b^{-16} + 228b^{-6} + 1.1b^{-2}], \quad (1)$$

where $\nu_0 = 6.32$ MHz (Turryshev & Anderson 2003). The actual deflection angle of a light ray grazing the Sun is the sum of $\theta_{\rm pl}(b,\nu)$ and the gravitational convergent deflection angle $\theta_{\rm gr}(b)$. Assuming that the spacetime around the Sun is well described by the Schwarzschild metric, $\theta_{\rm gr}(b)$ is given by

$$\theta_{\rm gr}(b) = \frac{4GM_\odot}{c^2 b R_\odot}, \quad (2)$$

where G is the gravitational constant, c is the speed of light, and $M_\odot$ is the solar mass (von Eshleman 1979). The opposite directions of the two deflection effects make the lensing impossible for frequencies below a critical value $\nu_{\rm crit}$ that depends on the impact parameter b. It can be computed with the following formula (Turryshev & Anderson 2003):

$$\nu_{\rm crit}(b) = \left[\nu_0^2 \frac{R_\odot c^2}{4GM_\odot}(2952b^{-15} + 228b^{-5} + 1.1b^{-1})\right]^{\frac{1}{2}}. \quad (3)$$

This formula gives $\nu_{\rm crit} = 64$ GHz for $b = 1.1$. Still, in practice, latitudinal dependencies and fluctuations in the coronal electron

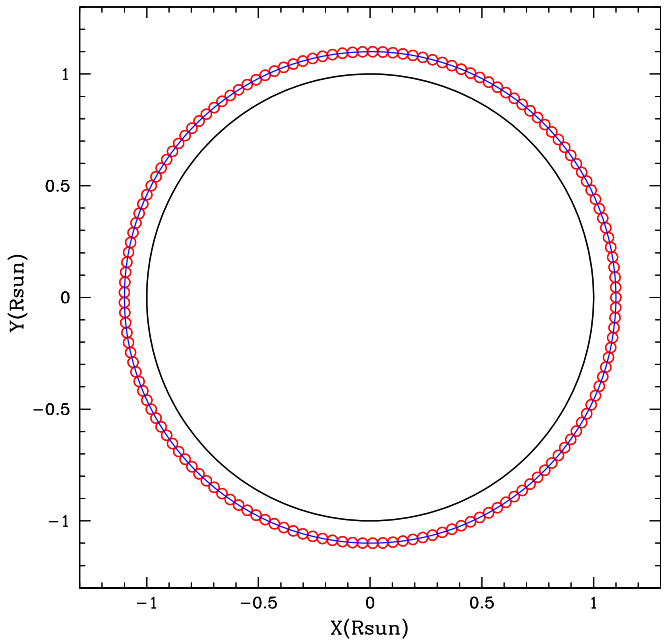

Figure 1. Illustration of the Sun (black circle) as seen from the hypothesized FICD. The blue circle represents the ER, i.e., the ring for which photons from the FICD will reach the target receptor. Its actual thickness is a few centimeters. The small red circles represent the laser beams emitted by the FICD in the Sun's plane. For this illustration, an impact parameter of 1.1 and a laser wavelength and waist of 500 nm and 1 m, respectively, were assumed. Each laser beam is ∼2.5 times wider than Earth.

density will strengthen the divergent effect of the coronal plasma, making it necessary to emit at frequencies beyond 1 THz (0.3 mm), to maximize the amplitude of the microlensing effect and to place the FICD at the shortest possible distance from the Sun (Turryshev & Anderson 2003). The microwave range used by classical SETI experiments (∼1–10 GHz) is thus not suited to a search for gravitationally focused extraterrestrial communications.

A second element to consider is the strong geometrical constraint for this special SETI strategy. Estimating it requires taking into account that, for a given distance to the Sun of the hypothesized FICD, only photons grazing the Sun within an extremely narrow Einstein ring (ER) around the Sun's disk will be focused to the targeted nearby star (e.g., von Eshleman 1979; Maccone 1994). Assuming a 100 m radius receiving antenna around Alpha Centauri A, we performed 2D ray-tracing computations based on Equations (1) and (2) for UV to IR wavelengths (see Appendix for a description of the methodology) that resulted in widths of a few centimeters for this ER. We thus assume here that, for the sake of efficiency, the assumed FICD transmitter is composed of an array of lasers emitting narrow Gaussian beams centered precisely on the ER (Figure 1), equivalent to a single more powerful laser emitting an annular beam sculpted to cover the ER. In this hypothesis, detecting an FICD's emission to a nearby star can only be done if the observer is within one of these narrow beams, putting a stringent geometrical constraint on the project concept. For an Earth-based observer, this means that Earth's minimum impact parameter has to be close to 1 as seen from the FICD and thus also from the targeted nearby star. In other words, Earth has to be a transiting (or nearly transiting) planet for one of the nearest stars to give this SETI concept a chance of success, so the target star has to be very close to the ecliptic plane. With its nearly circular orbit and its semimajor axis 215 times larger than the solar radius, Earth has a mean transit probability <0.5% for any random star of the solar neighborhood (Winn 2011). We can thus consider ourselves very lucky that the third-nearest stellar system, Wolf 359, a very low mass red dwarf of spectral type M6.0 V at a distance of 7.8 lt-yr (Jenkins et al. 2009; Sebastian et al. 2021), lies at only 0°.2 of the ecliptic plane, in the Leo constellation. For Wolf 359, Earth has a minimum impact parameter of about $215 \times \sin 0.^{\circ}2 = 0.75$, i.e., it is a transiting planet (Kaltenegger & Faherty 2021). Furthermore, Wolf 359 is a single star, i.e., it does not undergo strong dynamical perturbations that would make it necessary to change constantly the position of a putative FICD in its vicinity (Kerby & Wright 2021). These considerations make Wolf 359 an excellent target for a first attempt to detect an alien interstellar communication from the solar system.

Table 1
Communication Efficiency and Gain as Derived by 2D Ray-tracing Computations (see Annex 1 for Description) for Three Different GL-based Communication Strategies: Using the Sun only as a GL, Using Wolf 359 Only, or Using Both Stars

	Sun	Wolf 359	Sun + Wolf 359
Efficiency	$5.4e^{-9}$	$1.5e^{-10}$	$2.7e^{-9}$
Gain	$7.5e^{7}$	$2.1e^{6}$	$3.8e^{7}$

Note. In all cases, a power emission of 152 W was assumed.

A third element to consider is the sensitivity. To estimate it, we assumed the following parameters for the communication link from the solar system to Wolf 359:

1. The use of the Sun only as a GL. We performed again 2D ray-tracing computations (see Appendix) to estimate the extra gain that could be brought by using both stars or only Wolf 359 as GLs. Our results, in stark contrast with some previous papers (Maccone 2013, 2014), showed that the communication gain (relative to a non-GL laser communication) was a bit *smaller* when "closing the loop" and using also Wolf 359 as a GL, and significantly smaller when only Wolf 359 was used as a GL (see Table 1). We thus assumed that the putative alien probes would use the Sun only as a GL and would place the receptor around Wolf 359 at the location of their choice.
2. A mean emission wavelength of 500 nm (600 THz) for the lasers of the emitter. A much higher frequency than the lower limit of 1 THz mentioned above makes sense, so as to minimize the divergent impact of the Sun's corona. We adopted a wavelength of 500 nm for practicality purposes, as it lies in the optical range and the emission could then be detected by a ground-based telescope (as we attempted; see Sections 3.2 and 3.3).
3. A mass and radius of 0.11 $M_{\odot}$ and 0.14 $R_{\odot}$, respectively, for Wolf 359 (Sebastian et al. 2021).
4. An impact parameter b of 1.1 for the light rays grazing the Sun. For this impact parameter, our ray-tracing computations lead to a distance to the Sun of 663 au for the alien transmitter.
5. For the receptor around Wolf 359, a circular receptor with a radius $R_{\rm rec} = 100$ m.
6. For each laser, a waist (radius of the beam at its emission) of 1 m, corresponding thus to a space telescope with a 2 m diameter.

The Rayleigh length z_R of a laser is the distance from the emission source along the propagation direction corresponding to the doubling of the area of the beam's cross section. Assuming a Gaussian beam, it is given by

$$z_R = \frac{\pi\omega_0^2}{\lambda}, \quad (4)$$

where ω_0 is the laser waist (Svelto 2010). Under the assumed parameters, z_R is $\sim$6280 km $\sim 1\ R_\oplus$. The radius of the beam at a radial distance d from its source is then given by Svelto (2010):

$$\omega(d) = \omega_0\sqrt{1 + \frac{d^2}{z_R^2}}. \quad (5)$$

At 663 au, $\omega(d)$ is = 15,800 kms $\sim$2.5 $R_\oplus$, i.e., it could encompass Earth completely. To cover the whole ring of impact parameter 1.1 surrounding the Sun (Figure 1), an array of 152 lasers would be required. With bigger lasers (and thus smaller Rayleigh lengths), the beams would be narrower, so the global efficiency and the communication rate would be improved, but more lasers would be required to completely surround the Sun, resulting in an increase of the size but also of the mass of the FICD, and thus of the energy required to keep fixed its distance to the Sun. Of course, one could decide to use only a fraction of the ER. A balance has thus been found between the desired data transfer rate, the global efficiency of the FICD, its size, and its energetic consumption. In this respect, our assumed value of 1 m for the laser waist is nothing more than a simple work assumption to estimate the potential of detection of the FICD.

The global efficiency of the FICD is the fraction of the emitted photons that will actually reach the receptor. Our 2D ray-tracing computations (see Appendix) based on the assumptions described above enabled us to estimate a width of 13.3 cm for the ER. The FICD efficiency can be estimated as the inverse of the ratio of the area covered by a laser beam in the plane of the sky ($\pi \times (15.8e^6)^2$ m^2) and the fraction of it falling in the ER ($\sim 2 \times 0.133 \times 15.8e^6$ m^2). It leads to a value of $5.4e{-}9$, i.e., only $5.4e{-}7\%$ of the emitted photons will reach the receptor around Wolf 359. For comparison, one can compute that the efficiency of the same laser without using the Sun (or Wolf 359) as a GL is 7.15×10^{-17}. The resulting gain brought by the gravitational lensing is the ratio of these two efficiencies: $7.5 \times 10^7 = 78.8$ dB. This gain does not depend on the number of used lasers, i.e., whether the whole ER is covered or not.

At the core of the beam, the average intensity at a distance d from the beam waist $I_c(d)$ can be estimated as twice the total emission power P_0 divided by the area within the radius $\omega(d)$:

$$I_c(d) = 2 \times \frac{P_0}{\pi\omega^2(d)}. \quad (6)$$

Assuming an emission at a mean power of 1 W per laser (152 W in total then for the whole laser array), $I_c(d)$ is $\sim 2.6 \times 10^{-15}$ W m^{-2}, which corresponds to the intensity of a solar-type star of visual magnitude $\sim$17.6. The firm detection of such a source can be achieved within a few minutes of integration with a ground-based telescope with an aperture of a few dozen centimeters equipped with a modern CCD camera. Computing the motion of Earth relative to the Sun as seen from the FICD results in an average duration of 15 minutes for the crossing of the laser beam. Assuming exposures of 55 s without filter with the robotic 60 cm telescope TRAPPIST-South (Gillon et al. 2011; Jehin et al. 2011) at ESO La Silla, an effective seeing of 2″, the target at air mass 1.5, and the Moon at phase 0.5 and at 50° from the target's field of view, we computed a complete noise budget (read-out, dark, photon, scintillation, background) that led to an estimated signal-to-noise ratio of $\sim$200 for the detection of the emission after integration over the whole 15-minute beam crossing. We thus conclude that the hypothesized FICD targeting Wolf 359 could be detected with a modest-sized optical telescope like TRAPPIST-South, assuming that it emits constantly in the optical, even for very moderate emission powers.

3. Attempting to Detect an Interstellar Message from an Alien FICD: A First Try with TRAPPIST-South and SPECULOOS-South

Based on the considerations described above, we performed two searches for a GL-based communication from the solar system to Wolf 359. The first search was carried out in 2015 using the TRAPPIST-South telescope at ESO La Silla Observatory (Chile; Gillon et al. 2011; Jehin et al. 2011), and the second one was carried out in 2018 using the telescope Europa of the SPECULOOS-South facility at ESO Paranal Observatory (Chile; Burdanov et al. 2018; Delrez et al. 2018; Jehin et al. 2018; Sebastian et al. 2021). Both attempts were done during a transit of Earth as seen from the putative FICD (i.e., during an occultation of Earth as seen from Wolf 359). Both were done in the optical range. These observations and their analysis are described below (Section 3.2), but first we present the methodology used to compute the astrometric position of the FICD and its position relative to Earth during the observations.

3.1. Computation of the Astrometric Position of the FICD and Its Position Relative to Earth

Using as input the barycentric position (ICRS/J2016 system) and proper motion in R.A. (RA) and decl. (DEC) of Wolf 359 as measured by Gaia (early DR3 release; Gaia Collaboration et al. 2021), we computed the ICRS coordinates of Wolf 359 at the time of each observation. To the obtained R.A. and decl., we then added twice the product of the corresponding proper motion and the distance to Wolf 359 in light-years (Dly = 7.86 lt-yr) to compensate for the finite nature of the speed of light. Indeed, in that star's reference system, its astrometric position corresponds to the location it occupied Dly years ago. Furthermore, as a sniper aiming for a moving target, the FICD has to aim for the position that Wolf 359 will occupy Dly years from now (Figure 2). Given the high proper motion of Wolf 359, the amplitude of this correction is significant: $-59\farcs9$ and $-42\farcs4$ in R.A. and decl., respectively. Once this correction was made, the barycentric equatorial coordinates of the FICD were computed simply by removing/adding 180° from the obtained R.A. and decl. We did not consider aberration, as its effect is taken into account in the pointing model of the telescopes.

We then computed the FICD coordinates as seen from Earth and not from the Sun. First, a celestial transformation to the

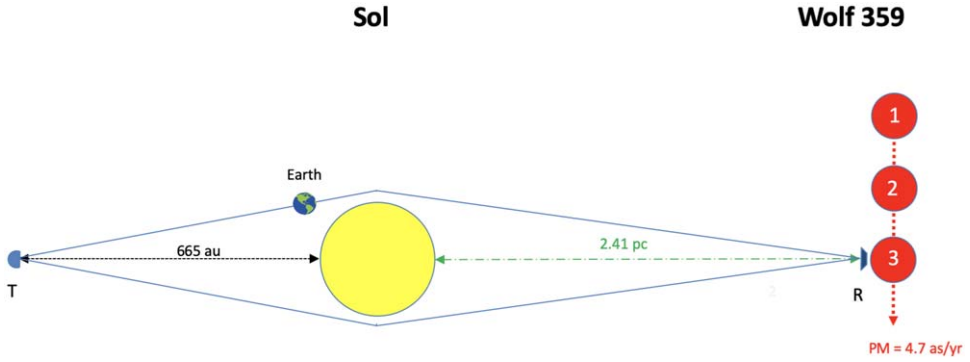

Figure 2. Illustration showing the geometry of the hypothesized communication link from the solar system to the Wolf 359 system. The distances and sizes are not to scale. Wolf 359 is shown at three different positions. Position 1 corresponds to the time of the emission of the photons that we receive from it now. Position 2 corresponds to its current position. Position 3 corresponds to the time at which it will receive the photons emitted now by the transmitter T (R = receptor).

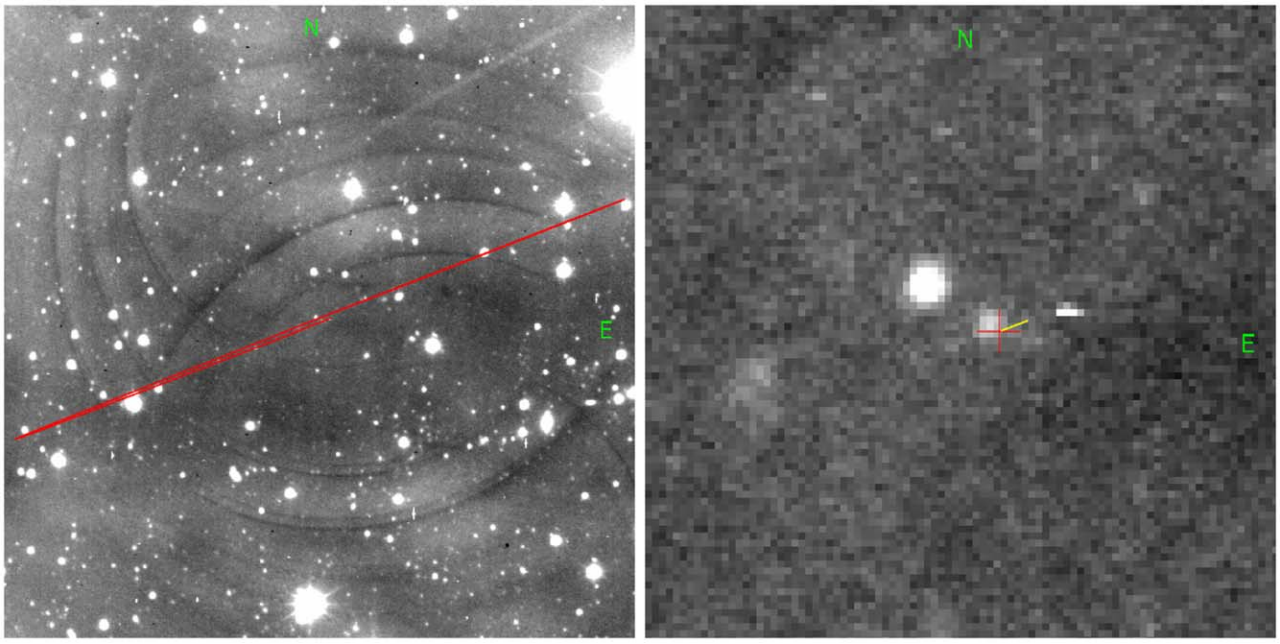

Figure 3. Left: 10′ by 10′ crop of the center of the stack (mean) of all images taken by TRAPPIST-South during the night of 2015 September 4–5. The position of the hypothetical FICD (under the assumptions of Section 2) between 2015 August 26 and 2016 August 26 is shown in red. This large motion on the sky is due the parallax effect combined with the compensation for the proper motion of Wolf 359. Right: 10″ by 10″ zoom-in on the path of the hypothetical FICD during the observations of TRAPPIST-South on 2015 September 4–5 (yellow line). The red plus sign shows the position that should have occupied the FICD at the inferior conjunction of Earth (i.e., in the middle of our planet's transit as seen from the FICD). The bright spot at the east of the FICD location is a hot pixel cluster.

ecliptic system was applied to the barycentric R.A. and decl. The ecliptic coordinates of the Sun at the time of each observation were then computed, providing all the inputs required to move to a geocentric system. A reverse transformation to the equatorial system led finally to the geocentric R.A. and decl. of the FICD at the time of each observation. For each observation, we also used the ecliptic positions of the FICD and the Sun to compute the distance between the center of Earth and the center of the Sun on the plane of the sky as seen from the FICD (see Figures 3 and 5), so as to predict the entering of Earth into and exiting of Earth out of the FICD beam under an assumed communication strategy (impact parameter, wavelength, laser waist).

3.2. TRAPPIST-South Observations

TRAPPIST-South is a 60 cm robotic telescope located at La Silla Observatory (Chile) and dedicated to the observation of exoplanet transits and small bodies of the solar system (Gillon et al. 2011; Jehin et al. 2011). It has a Ritchey–Chretien design and is coupled to a German equatorial mount. It is equipped with a thermoelectrically cooled 2k × 2k CCD camera with a field of view of 22′ × 22′ (pixel scale = 0.″65) and a quantum efficiency larger than 50% from 300 to 920 nm. Pointing on the ICRS coordinates R.A. = $22^{h}56^{m}20\overset{s}{.}81$ and decl. = $-06^{d}59^{m}28\overset{s}{.}3$ (computed as described in Section 3.1), TRAPPIST-South observed during the whole night of 2015 September 4−5, from $23^{h}24$ UT to $10^{h}13$ UT, which corresponded to the start of the transit of Earth as seen from the putative FICD (Figure 3). To ease the confirmation of a putative extra source in the images of the night, the same field was observed again on September 5 and 8 for a few hours. All these observations were carried out without any filter, so as to provide a spectral coverage as wide as possible (from ∼300 to 950 nm). An exposure time of 55 s was used for all images. A total of 536 images were taken on 2015 September 4, and 140 and 152 were taken on September 5 and 8, respectively.

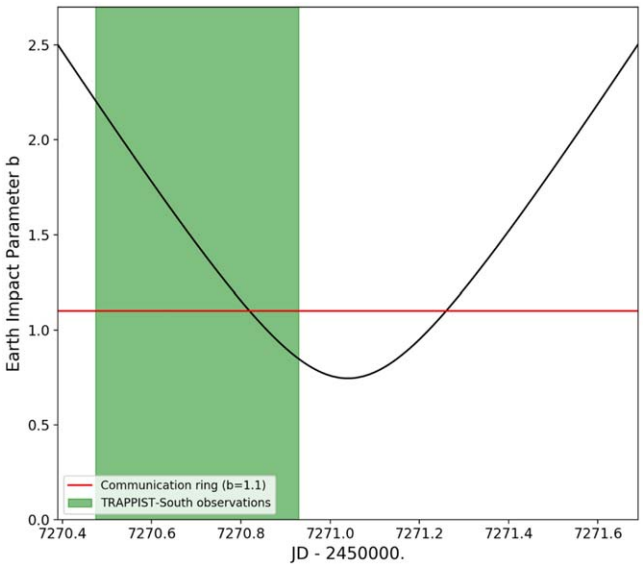

Figure 4. Evolution of the impact parameter of Earth as seen from the "solar gravitational line" (SGL) of Wolf 359 around the TRAPPIST-South observations of 2015. The red line corresponds to an impact parameter of 1.1. The green zone corresponds to the TRAPPIST-South observations. The intersection of the red and black lines corresponds to the crossing of the putative FICD's beam by Earth.

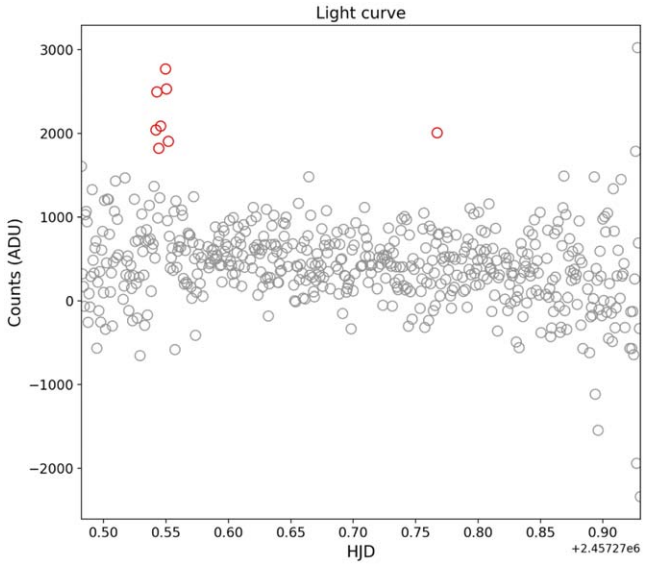

Figure 5. Sky-subtracted light curve of the source located approximately at the position of the hypothetical FICD in the TRAPPIST-South images. The points in red have a significant flux excess. The first group of red points is due to the passage of a $g \sim 19.5$ asteroid in the aperture. We attributed the other outlier to a cosmic hit.

For the three runs, a standard pre-reduction (bias, dark, flat-field correction) was applied to the images, and then they were aligned and combined. The resulting high signal-to-noise ratio stack image was then plate-solved, and the expected position of the FICD was overplotted (Figure 3). Comparing the stacked image of the first night to the ones of the second and third nights, a visual search for an extra source in the expected position range of the FICD was performed. No extra source could be identified.

Figure 4 shows the evolution of the Earth–Sun distance on the plane of the sky during the night of 2015 September 4 as seen from the putative FICD. Assuming a focal impact parameter of 1.1, i.e., to an ER with a radius of 1.1 $R_\odot$ (corresponding to an FICD–Sun distance of 663 au; see above), Earth should have crossed this ring around 2,457,270.82 JD = 7^h40 UT. Under our assumptions on the laser waist described in the previous section, and taking into account Earth's orbital speed of $\sim$30 km s^{-1}, the telescope should have remained in the laser beam for $\sim$8 minutes. Still, this simple estimate neglects the fact that, as seen from the FICD, Earth's transit has a high impact parameter (0.73), and so Earth's path is nearly tangential to the focal annulus, which results in a much longer time within the beam of $\sim$25 minutes. Based on this estimate, we combined the images of the night 10 by 10 and inspected the resulting stacked images in search of an extra source appearing at the expected position range of the FICD for one or a few of them. We could not detect any transient extra source, but we noticed that a very faint source (estimated g magnitude $\sim$22) was located at the ICRS coordinates R.A. 22:56:20.77, decl. −06:59:28.4, which corresponds approximately to the position expected for the FICD during Earth's transit (Figure 4). Nevertheless, this source is also present in the stacked images of the two other TRAPPIST-South runs, while the FICD should have been at other positions because of its large parallactic motion (see Figure 3). Furthermore, if this source had been the searched FICD, it should have drifted significantly on the sky during the night of 2015 September 4–5 (see Figure 3), again because of its large parallax, which was not the case.

To ensure that this faint source could not have hidden the emission of the hypothetical FICD, we studied its photometric stability. For that purpose, we used IRAF/DAOPHOT (Stetson 1987) to extract the fluxes within a circular aperture with a radius of 6 pixels (4″) centered on its position in the stacked image of the night. As this star is too faint to be visible in individual images, we fixed the position of the center of the aperture. We measured the background in an annulus extending from 18 to 28 pixels from the center of the aperture. Figure 5 shows the resulting light curve. In addition to an increase of the scatter at the beginning and at the end of the night, one can notice several outliers with a significant flux excess. Examining the individual images and a movie of them, we noticed that the first group of outliers corresponds to the passage of an asteroid ($g \sim 19.5$) right in the aperture. The other outlier corresponds to a cosmic hit.

In a last step, we used the mean g magnitude of the faintest stars registered in the Gaia early DR3 catalog visible in the images stacked 10 by 10 to estimate the highest visual magnitude for which a source would have been detected by visual inspection. We reached a value of 21.8, much larger than the magnitude of 18.3 that we estimated under the assumptions described in Section 2. This magnitude corresponds to the one of the source at R.A. 22:56:20.77, decl. −06:59:28.4. This leads us to the conclusion that our observations had the sensitivity to detect the communication of the putative FICD to Wolf 359 under the assumptions described in Section 2.

3.3. SPECULOOS-South Observations

SPECULOOS-South is a facility composed of four 1 m robotic telescopes located at Paranal Observatory, Chile (Burdanov et al. 2018; Delrez et al. 2018; Jehin et al. 2018). It is the core facility of the SPECULOOS project that aims to explore all nearby ultracool dwarf stars (spectral type later than

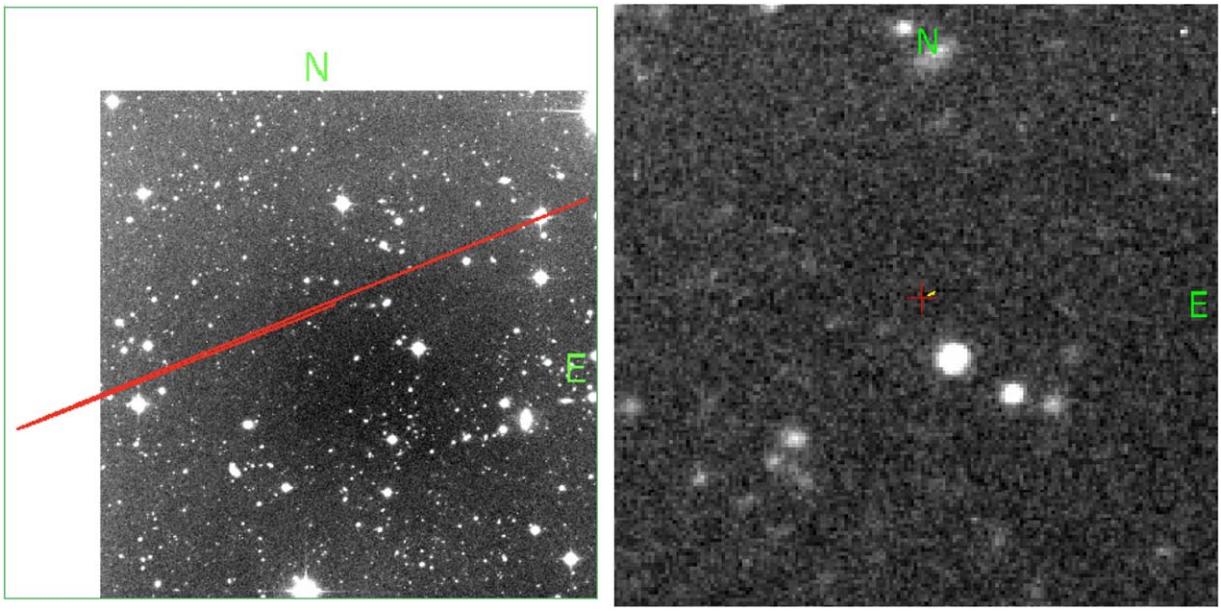

Figure 6. Same as Figure 3, but for the 150 first images taken by SPECULOOS-South/Europa of 2018 September 4–5. The whole stack of the images (left) is smaller than $10' \times 10'$ because of the shift of the images due to the tracking problem experienced by the telescope during the night.

M6) within 40 pc for transiting planets (Gillon 2018; Sebastian et al. 2021). Each of its four telescopes has a Ritchey−Chretien design and is mounted on an equatorial mount with a special design making it unnecessary to flip the telescope position at meridian. All telescopes are equipped with a thermoelectrically cooled deep-depletion 2k × 2k camera with a field of view of $12' \times 12'$ (pixel scale = $0''.35$) and a quantum efficiency larger than 50% from 420 to 950 nm. The SPECULOOS-South telescope Europa observed the whole night of 2019 September 4−5, from 0 h UT to 9^h24 UT, which corresponded to the start of the transit of Earth as seen from the putative FICD. All these observations were carried out without any filter, so as to provide a spectral coverage as wide as possible. An exposure time of 50 s was used for the 492 taken images.

The same reduction and analysis procedures as for the TRAPPIST-South data were applied. During the reduction, we noticed that the tracking of the telescope performed poorly during the night because of the use of a bad pointing model (at that time, the telescope was still in commissioning phase). Because of this bad tracking resulting in a shift of the stars of $\sim 1''$ from one image to the other, we had to discard all images taken after 2^h55 UT, keeping only the first 150 images. Fortunately, the crossing of the ER by Earth was supposed to take place within the first 3 hr of the night, with a start of the transit of Earth as seen from the FICD computed to happen around 1^h45 UT (Figure 6).

As for TRAPPIST-South, we examined the individual images and the images stacked 10 by 10. We did not find an extra source at the expected position of the FCID in any of those images (Figures 6 and 7 are the SPECULOOS counterparts of Figures 3 and 4).

Using the same method as for the TRAPPIST-South observations, we estimated the highest g-band magnitude for which a source would have been detected by visual inspection of the images stacked 10 by 10. We reached a value of 22.5, high enough to ensure that the putative FICD would have been detected under the assumptions described in Section 2.

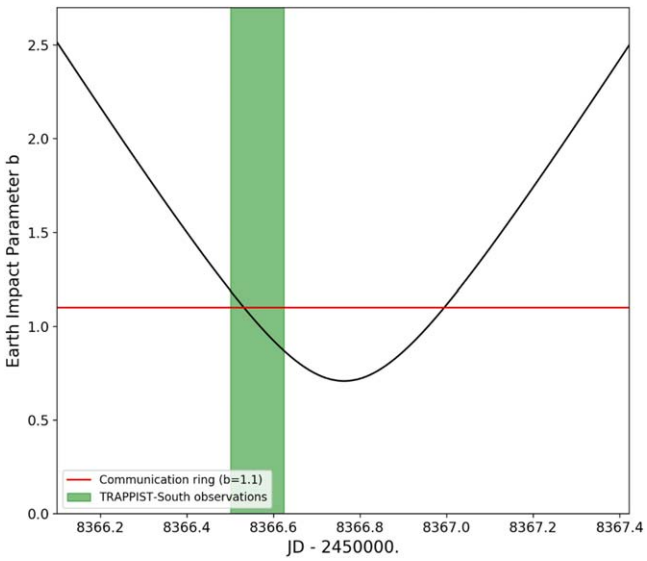

Figure 7. Evolution of the impact parameter of Earth as seen from the hypothetical FICD around the SPECULOOS-South observations of 2018. The red line corresponds to an impact parameter of 1.1. The green zone corresponds to the SPECULOOS-South observations.

4. Discussion

This search for an interstellar optical communication from the solar system to Wolf 359 did not lead to any detection. Assuming that the searched FICD does exist and emits constantly toward Wolf 359 in the optical range and that we were in its beam, because it beamed into either the entire ER or just a portion that contained Earth, our derived upper limits on its g magnitude (21.8 for TRAPPIST-South and 22.5 for SPECULOOS-South; see previous section) correspond to stringent upper limits on its total emitting power of 3.2 and 1.7 W (0.02 and 0.01 W per laser).

As usual for SETI null results, our nondetection could be explained by a large collection of alternative hypotheses: our solar system had never been reached by the probes from an

alien technological civilization; such probes are well in our solar system, but they do not use a GL-based communication strategy; they do use this strategy, but they did not establish a communication link between the solar and the Wolf 359 system; such a link exists, but the corresponding alien FICD did not emit during our observations; it did, but it always avoided one of its beams passing on Earth to remain hidden to the local young technological civilization; it does not use optical wavelengths for its message to Wolf 359; etc.

Assuming that the searched-for alien FICD does exit and emits continuously, one could wonder whether the assumptions presented in Section 2 represent the optimal strategy for such interstellar communication. First, one could wonder whether the assumed setup, i.e., using the Sun only as a GL, is optimal. If we consider the alternatives of using Wolf 359 instead of the Sun, or using both stars, the results of our 2D ray-tracing computations (see Table 1) show that it is indeed the best strategy in terms of communication gain. While using both stars would result in a gain twice as small, the use of Wolf 359 only would result in a gain more than 60 times smaller. But this would mean that the receptor around Wolf 359 would have to point toward the Sun. At such a distance (∼7.8 lt-yr), the angular separation between the ER and the Sun's disk would be ∼390 μas, making the masking/nulling of the Sun's disk while preserving the ER's signal an extremely challenging technological problem. Nevertheless, this problem is much less severe if one considers the use of lasers for the signal emission. Indeed, as outlined by many works on optical SETI (e.g., Horowitz et al. 2001), the monochromatic and pulsed nature of lasers enables us to compress the signal frequency and/or time and to select a wavelength corresponding to a strong stellar absorption line (even if very narrow), so as to have it standing out easily against the stellar photons.

One could also question our choice of the optical range for the communication. This choice was observational, i.e., it was mostly dictated by our capacity to detect the putative emission with our optical ground-based telescopes. From a purely theoretical point of view, a shorter wavelength range (UV) could be better suited for the task, at it would minimize even further scattering of the signal by the solar corona (Equation (1)) while increasing the efficiency of the communication by narrowing the size of the laser beams. On the other side, for the same available energy, using extremely high frequencies for the emitted photons (X and γ ranges) could negatively impact the possible complexity of the signal, as fewer photons would be emitted per second. Based on these considerations, it would be desirable to reproduce this SETI experiment in the UV, which would require the use of a space-based (or a balloon-based) telescope.

Another element to consider is the radial position of the emitting probe relative to the Sun. In Section 2, we made the assumption that it was composed of an array of 1 m waist lasers located in-focus at a computed distance to the Sun of 663 au. Nevertheless, nothing prevents these emitters from being separated and independent, as well as off-center relative to the focal line (Figure 8). In such a case, they could be much closer to the Sun, which would bring two important advantages: their beams in the Sun's plane would be significantly narrower, and they would receive much more energy from the Sun per second. Nevertheless, there would be a price to pay. Indeed, the light rays emitted by the laser would reach the Sun's plane with a different angle, except for those at

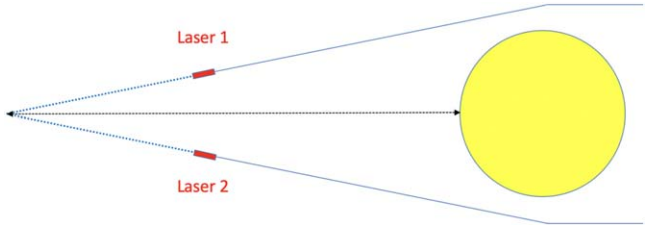

Figure 8. Illustration of off-axis FICDs located closer to the Sun than the SGL.

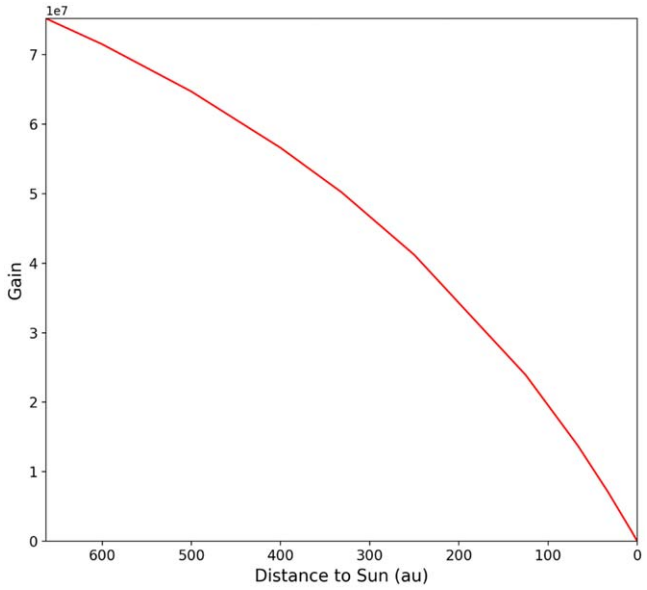

Figure 9. Communication gain relative to a non-GL emission as a function of distance between the emitter and the Sun (663 au = in-focus), as computed from ray-tracing simulations under the assumptions described in the text.

the exact center of the beam. Performing new 2D ray-tracing computations confirmed a decrease of the gain for larger distances to the focus (Figure 9). Still, the gain remains significant down to very small distances to the Sun, and it is more than compensated by the increase of the solar irradiation with smaller distance. For instance, putting the emitter at the distance of 10 au makes the ER's width (and thus the gain) shrink by a factor 33, while the stellar irradiation of the FICD would increase by a factor 4400. A point to consider as well is that parking the FICD closer to the Sun would also lead to stronger gravitational perturbations from the planets that would require more axial position corrections, and thus more energy, to keep the FICD-Sun-target alignment (Kerby & Wright 2021). A possibly interesting option could be to place the FICD close to the outer edge of the Kuiper Belt, to avoid too strong gravitational perturbations from giant planets while remaining relatively close to a source of raw material (which could be necessary to maintain the emitter in operational state over thousands if not millions of years) and benefiting from a solar irradiation still ∼100 times larger than at the SGL.

Based on all the considerations above, we performed new 2D ray-tracing computations (see Appendix), this time assuming one single laser (and not the full array required to cover the whole EC) emitting with a power of 1 W at 50 nm with a waist of 1 m at a distance of 66.3 au from the Sun. They led to 2.5e9 photons reaching the 100 m radius receptor around Wolf 359 per second, to be compared to $\sim 1.35 \times 10^{10}$ photons

per second computed assuming an in-focus laser operating at 500 nm. This modest decrease by a factor 5 of the received flux relative to an in-focus position could be more than balanced by the 100 times larger irradiation of the FICD.

This alternative hypothesis assuming an FICD composed of one to several off-center lasers located closer to the Sun makes less appealing the search strategy used in this work, as it would be highly unlikely that Earth would pass in the narrow communication beam(s) of one of these few probes. Nevertheless, their closer distance to the Sun could make possible their direct detection in reflected light. G14 computed a value of 30.5 for the optical magnitude of an FICD with a payload of 1 ton and a sail surface density of 0.5 g m^{-2} located at 550 au. This estimate was an absolute lower limit, as it assumed the sail to be seen with a zero phase angle (i.e., from Earth transiting the Sun as seen from the FICD), a Bond albedo of 1, and a purely specular reflection. Assuming now a heliocentric distance of 50 au, this estimated magnitude would shrink to a value of 25.3, which is still out of reach of a 1 m class telescope like those used in this work, but well within reach of the biggest existing telescopes. For instance, we used the online Exposure Time Calculator of the FORS2 instrument of the ESO Very Large Telescope[4] to compute a signal-to-noise ratio of 12 on a $V = 25.4$ target, assuming a 1 hr exposure in Bessel R filter and average observing conditions (air mass 1.5, Moon illumination 0.5). In reality, a solar sail would not have a perfectly specular reflection (even if built by more technologically advanced aliens), so its actual magnitude should be a bit higher, but it could be compensated by observing without any filter, using a bigger telescope like the upcoming E-ELT, using adaptive optics to boost the contrast with the sky background, etc.

It should also be noted that assuming such an off-center architecture for the FICD increases significantly the uncertainty on the possible positions of its laser+sail components. Assuming an impact parameter of 1.1, a central transit of Earth as seen from the GL focal point, and a distance to the Sun of 50 au for its components, the surface to explore would not be a point anymore but a circle of radius of $\sim 0\farcm65 = 39''$. Furthermore, 50 au for the distance is just an arbitrary value. The laser(s) could be farther away, but they could also be much closer to the Sun, making it necessary to explore a much larger field of view (but easing the detection in terms of signal-to-noise ratio).

While the detailed study of the potential for the direct detection of such an FICD composed of off-center laser+sail units is beyond the scope of this paper, we performed a first search based on this hypothesis in our data. This search for faint moving targets was done using a synthetic tracking (or "shift-and-add") algorithm, a powerful and computationally expensive method for searching for moving objects in astronomical images by stacking the images according to all the possible movements of the object (see, e.g., Cochran et al. 1995; Shao et al. 2014). To perform this search, we used the Tycho Tracker[5] software, restricting the search to objects moving slower than $0\farcs5$ $minute^{-1}$. Upon completion of the search, we could not reliably identify any objects that move slower than $0\farcs5$ $minute^{-1}$ and that are brighter than our estimated sensitivity upper limit of g magnitude $\sim$23.5. This limit would correspond to a 1 ton (payload) FICD located at $\sim$20 au, close to the orbit of Uranus.

Unlike our attempt presented here to detect the communication from a putative alien FICD to Wolf 359, the search for the reflected light signal from off-axis FICD does not necessarily require the FICD (and thus its target star) to lie in the ecliptic. Based on this fact, we have decided to perform a search sensitive to objects up to magnitude $\sim$26 for the 10–20 nearest stars. This search is ongoing, and its results will be presented in a forthcoming paper.

TRAPPIST-South is funded by the Belgian Fund for Scientific Research (Fond National de la Recherche Scientifique, FNRS) under the grant FRFC 2.5.594.09.F, with the participation of the Swiss National Science Fundation (SNF). SPECULOOS-South has received funding from the European Research Council under the European Union's Seventh Framework Programme (FP/2007-2013; grant agreement No. 336480/SPECULOOS) and under the 2020 research and innovation program (grant agreement No. 803193/BEBOP), from the Balzan Prize Foundation, from the Belgian Scientific Research Foundation (F.R.S.-FNRS; grant No. T.0109.20), from the University of Liege, from the ARC grant for Concerted Research Actions financed by the Wallonia-Brussels Federation, from the Simons Foundation (PI D. Queloz, grant No. 327127), from the MERAC foundation, and from the Science and Technology Facilities Council (STFC; grant No. ST/S00193X/1). M.G. is FNRS Research Director.

Appendix
2D Ray-tracing Computations

Under the thin-lens and circular symmetry hypotheses, the following 2D geometrical approach can be used to compute the efficiency and gain of a GL-based communication link.

A.1. Using Two Stars as GLs

Figure 10 shows a 2D representation of the geometry of the communication link between the two stars, under the thin-lens approximation. The transmitter (T), the first star (S1), the second star (S2), and the receptor (R) are all located on the same line, with d_{T-S1} the distance between the transmitter and the first star, d_{S1-S2} the distance between the two stars, and d_{S2-R} the distance between the second star and the receptor. For a selected impact parameter b, the orthogonal distances y_1 and y_2 are bR_1 and bR_2, respectively, where R_1 and R_2 are the radii of both stars. The other geometrical elements of the communication link can be derived using

$$\alpha_2 = \arctan(y_1 - y_2)/d_{S1-S2} \quad \text{(A1)}$$

$$\alpha_1 = \alpha_{dev1} - \alpha_2 \quad \text{(A2)}$$

$$\alpha_3 = \alpha_{dev2} + \alpha_2 \quad \text{(A3)}$$

$$d_{T-S1} = y_1/\tan\alpha_1 \quad \text{(A4)}$$

$$d_{S2-R} = y_2/\tan\alpha_3, \quad \text{(A5)}$$

where the deviation angles α_{dev1} and α_{dev2} are the sums of the gravitational and scattering deviation angles for star 1 and star 2 as computed with Equations (1) and (2) and assuming an impact parameter b.

At this stage, we fix the radial positions of the transmitter and receptor (d_{T-S1} and d_{S2-R}), and we add small increments to $y1$ in both directions, i.e., $y_1' = y_1 + \delta_{y1}$, iterating on δ_{y1} until the

[4] https://www.eso.org/observing/etc/bin/simu/fors_ima
[5] https://www.tycho-tracker.com

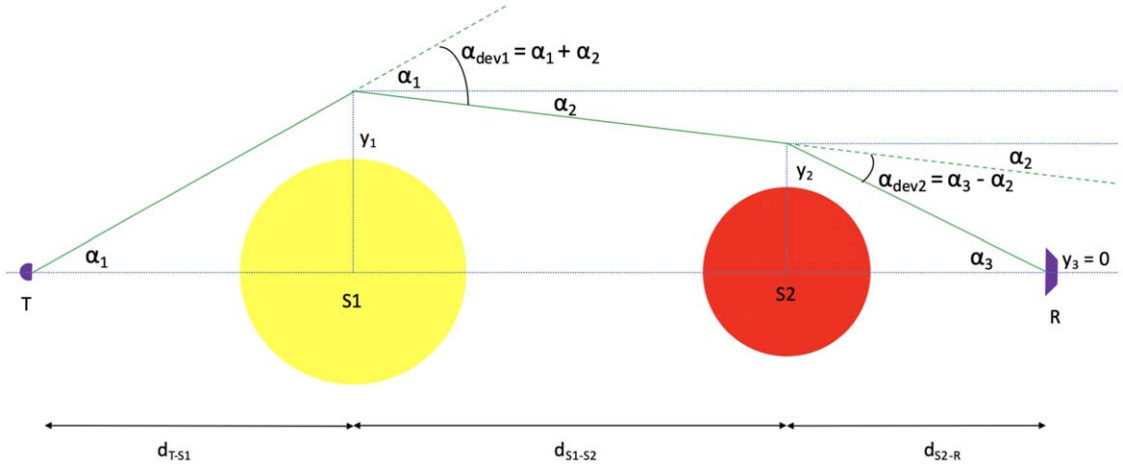

Figure 10. Illustration showing the geometry of the GL communication link assuming that both stars S1 and S2 are used as GLs. See text for details.

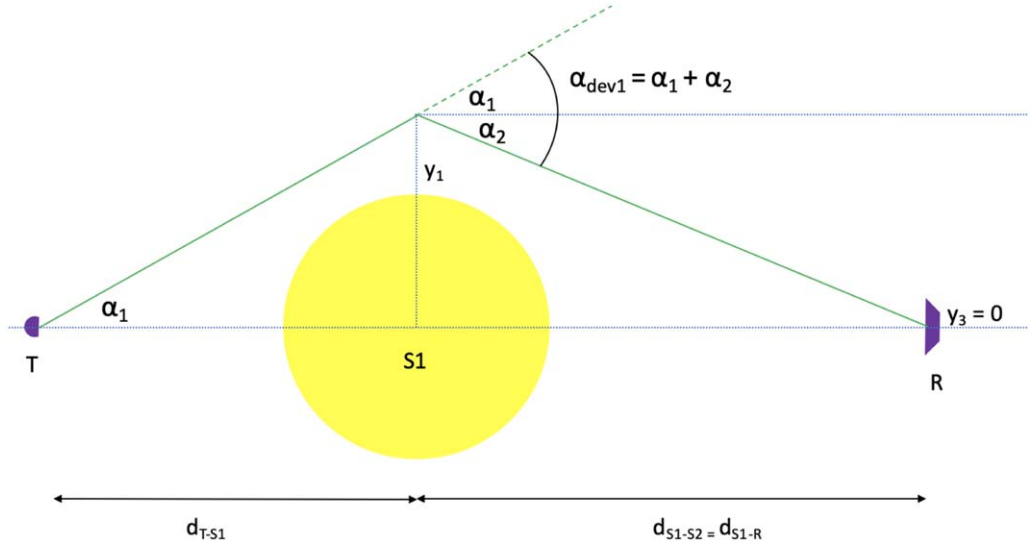

Figure 11. Illustration showing the geometry of the GL communication link assuming that only star S1 is used as a GL. See text for details.

computed ray does not intersect with the receptor R anymore. For each tried value of y_1', α_1' (from Equation (A16)) and α_{dev1}' (from Equations (1) and (2)) are computed, and then α_2' (Equation (A9)), y_2' (Equation (A1)), α_{dev2} (Equations (1) and (2)), and α_3' (Equation (A12)). Finally, the vertical position y_3' of the light ray at the radial position of the receptor R is computed as

$$y_3^{'} = y_2^{'} - d_{S2-R} \tan \alpha_3^{'}. \tag{A6}$$

If $|y3'|$ is smaller than or equal to the assumed radius of the circular receptor R_R, then the emitted photon is considered to be detected.

By iterating on y_1', one obtains the width of the ER W_{ER}. Assuming that the intensity in the laser beam is homogeneous, we can then compute the efficiency of the communication link $E_{CL(GL)}$ (i.e., the fraction of emitted photons reaching the detector) by using the equation

$$E_{CL(GL)} = \frac{2W_{ER}\omega(d_{E-S1})}{\pi\omega(d_{E-S1})^2}, \tag{A7}$$

where $\omega(d_{E-S1})^2$ is given by Equation (5).

To compute the gain, one has to compute the communication efficiency without $GE_{CL(wt-GL)}$ (i.e., the fraction of photons emitted by the laser that reach the receptor R without using any star as GL) using the equation

$$E_{CL(wt-GL)} = \frac{\pi R_R^2}{\pi\omega(d_{S1-S2})^2}, \tag{A8}$$

where $\omega(d_{S1-S2})^2$ is again given by Equation (5).

The ratio of the efficiencies $E_{CL(GL)}$ and $E_{CL(wt-GL)}$ gives finally the gain of the GL link.

A.2. Using only Star 1 as a GL

In the case in which only star 1 is used as GL (i.e., the star hosting the transmitter T), the 2D geometry of the communication link becomes the one shown in Figure 11. The geometric relationships to use are then

$$\alpha_2 = \arctan(y_1)/d_{S1-S2} \tag{A9}$$

$$\alpha_1 = \alpha_{dev1} - \alpha_2 \tag{A10}$$

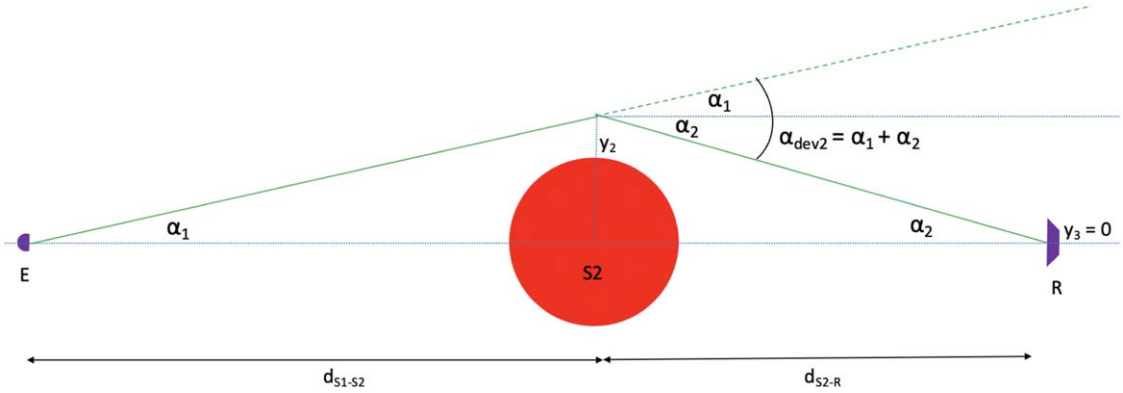

Figure 12. Illustration showing the geometry of the GL communication link assuming that only star S2 is used as a GL. See text for details.

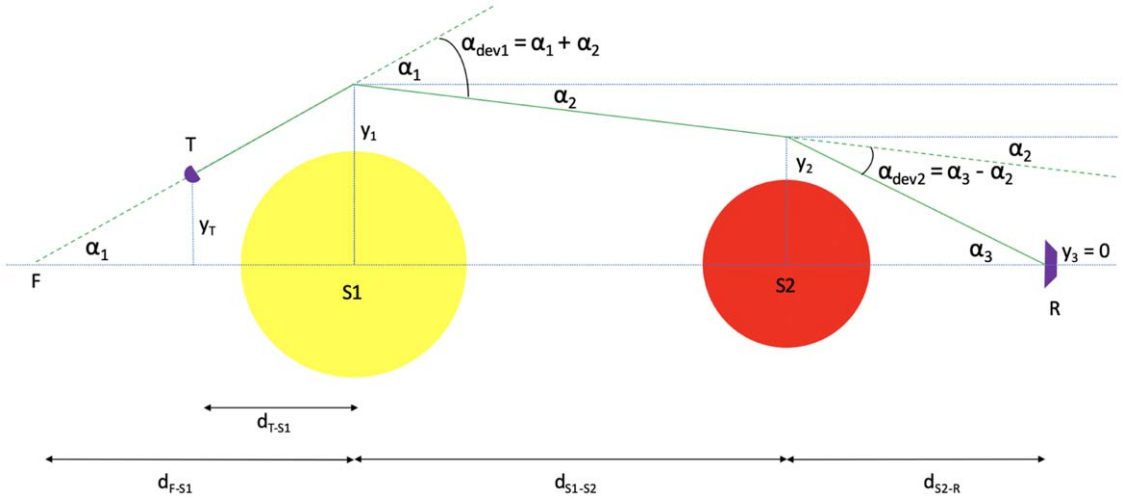

Figure 13. Illustration showing the geometry of the GL communication link assuming that both stars S1 and S2 are used as GLs and the transmitter T is placed closer to S1 and off-axis (relative to the SGL). See text for details.

$$d_{\mathrm{T-S1}} = y_1/\tan\alpha_1. \quad \text{(A11)}$$

The methodology to compute W_{ER} and $E_{\mathrm{CL(GL)}}$ is the same as in the previous case.

A.3. Using only Star 2 as a GL

In the case in which only star 2 is used as a GL (i.e., the star hosting the receptor R), the 2D geometry of the communication link becomes the one shown in Figure 12. The geometrical relationships to use are then

$$\alpha_1 = \arctan(y_2)/d_{\mathrm{S1-S2}} \quad \text{(A12)}$$

$$\alpha_2 = \alpha_{\mathrm{dev2}} - \alpha_1 \quad \text{(A13)}$$

$$d_{\mathrm{S2-R}} = y_2/\tan\alpha_2. \quad \text{(A14)}$$

The methodology to compute W_{ER} and $E_{\mathrm{CL(GL)}}$ is the same as in the previous cases, except that the width of the laser beam has to be computed for the distance $d_{\mathrm{S1-S2}}$.

A.4. Off-axis Transmitter

If one assumes that the transmitter is placed closer to S1 and off-axis (relative to the SGL), and assuming that both stars are used as GLs, the geometry of the communication link becomes the one shown in Figure 13. First, the radial position of the focus relative to S1, $d_{F-\mathrm{S1}}$, is computed as in case A.1. For a selected radial distance $d_{\mathrm{T-S1}}$ of the transmitter T relative to star S1, its orthogonal position y_{T} is then computed via

$$y_{\mathrm{T}} = (d_{F-\mathrm{S1}} - d_{T_{\mathrm{S}}1})\tan\alpha_1. \quad \text{(A15)}$$

The radial distance of the receptor R relative to S2 is also computed as in case A.1. Then, to estimate the width of the ER W_{ER}, one has to take into account that the light rays will emanate from an off-focus position as shown in Figure 14. Given y_1', α_{dev1}' is computed using Equations (1) and (2), and then α_1', α_2', and y_2' are computed through

$$\alpha_1' = \arctan(y_1' - y_{\mathrm{T}}')/d_{\mathrm{T-S1}} \quad \text{(A16)}$$

$$\alpha_2' = \alpha_{\mathrm{dev1}}' - \alpha_1' \quad \text{(A17)}$$

$$y_2' = y_1' - d_{\mathrm{S1-S2}}\tan\alpha_2'. \quad \text{(A18)}$$

Parameter α_{dev1}' is then computed using Equations (1) and (2), and then α_3' and y_3' are computed using

$$\alpha_3' = \alpha_{\mathrm{dev2}}' + \alpha_2' \quad \text{(A19)}$$

$$y_3' = y_2' - d_{\mathrm{S2-R}}\tan\alpha_3'. \quad \text{(A20)}$$

The computation of the communication efficiency and the gain are as in case A.1. The same methodology applies to the cases where only S1 or S2 is used as a GL.

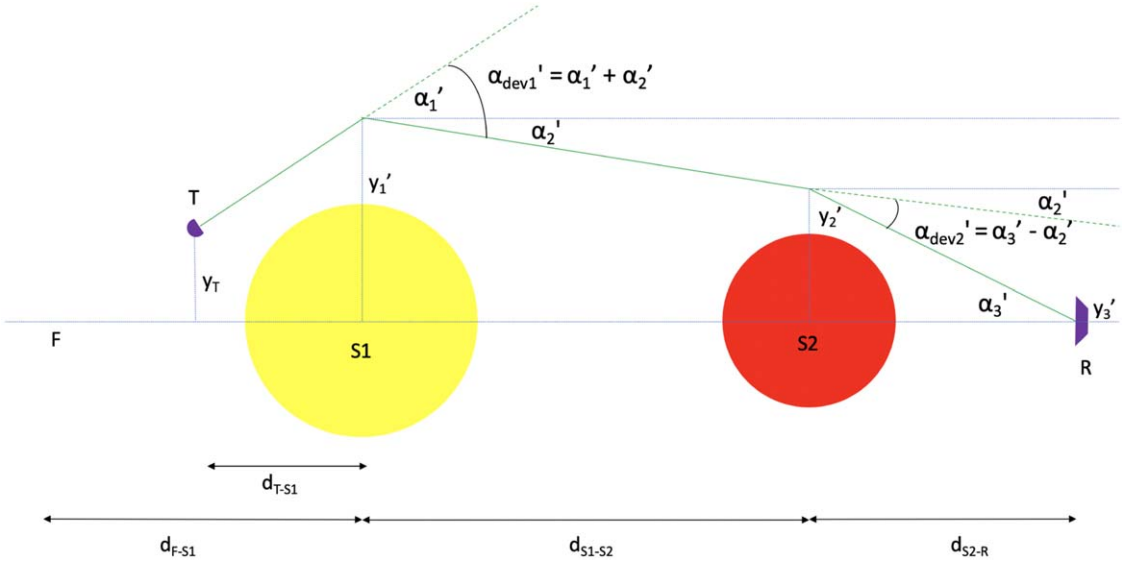

Figure 14. Same as Figure 13, but for a slightly different impact parameter of the light ray, so as to illustrate how the width of the ER is computed.

ORCID iDs

Michaël Gillon https://orcid.org/0000-0003-1462-7739
Artem Burdanov https://orcid.org/0000-0001-9892-2406
Jason T. Wright https://orcid.org/0000-0001-6160-5888

References

Burdanov, A., Delrez, L., Gillon, M., & Jehin, E. 2018, in Handbook of Exoplanets, ed. H. J. Deeg & J. A. Belmonte (Berlin: Springer), 130
Cochran, A. L., Levison, H. F., Stern, S. A., & Duncan, M. J. 1995, ApJ, 455, 342
Delrez, L., Gillon, M., Queloz, D., et al. 2018, Proc. SPIE, 10700, 107001I
Freitas, R. A. 1980, JBIS, 33, 251
Gaia Collaboration, Brown, A. G. A., Vallenari, A., et al. 2021, A&A, 649, A1
Galea, P., & Swinney, R. 2011, JBIS, 64, 24
Gertz, J. 2018, JBIS, 71, 375
Gertz, J. 2021, JBIS, 71, 427
Gillon, M. 2014, AcAau, 94, 629
Gillon, M. 2018, NatAs, 2, 344
Gillon, M., Jehin, E., Magain, P., et al. 2011, EPJ Web Conf., 11, 06002
Hippke, M. 2020a, arXiv:2009.01866
Hippke, M. 2020b, AJ, 159, 85
Hippke, M. 2021, arXiv:2104.09564
Horowitz, P., Coldwell, C. M., Howard, A. B., et al. 2001, Proc. SPIE, 4273, 119
Jehin, E., Gillon, M., Queloz, D., et al. 2011, Msngr, 145, 2
Jehin, E., Gillon, M., Queloz, D., et al. 2018, Msngr, 174, 2
Jenkins, J. S., Ramsey, L. W., Jones, H. R. A., et al. 2009, ApJ, 704, 975
Kaltenegger, L., & Faherty, J. K. 2021, Natur, 594, 505
Kerby, S., & Wright, J. T. 2021, AJ, 162, 252
Maccone, C. 1994, JBIS, 47, 45
Maccone, C. 2013, AcAau, 82, 246
Maccone, C. 2014, AcAau, 104, 458
Marcy, G. W., Tellis, N. K., & Wishnow, E. H. 2022, MNRAS, 509, 3798
Sebastian, D., Gillon, M., Ducrot, E., et al. 2021, A&A, 645, A100
Shao, M., Nemati, B., Zhai, C., et al. 2014, ApJ, 782, 1
Stetson, P. B. 1987, PASP, 99, 191
Svelto, O. 2010, Principles of Laser (5th edn.; Berlin: Springer)
Tarter, J. 2001, ARA&A, 39, 511
Turryshev, S. G., & Anderson, B.-G. 2003, MNRAS, 341, 577
Valdes, F., & Freitas, R. A. 1980, JBIS, 33, 402
von Eshleman, R. 1979, Sci, 205, 1133
Winn, J. N. 2011, in Exoplanets, ed. S. Seager (Tucson, AZ: Univ. Arizona Press), 55